Journal of Statistical Physics, Vol. 94, Nos. 5/6, 1999

Neural Networks in Which Synaptic Patterns Fluctuate with Time

J. Marro,[1] J. J. Torres,[1, 2] and P. L. Garrido[1]

Received July 9, 1998; final October 19, 1998

We study a stochastic neural-network model in which neurons and synapses change with *a priori* probability p and $1-p$, respectively, in the limit $p \to 0$. This implies neuron activity competing with fast fluctuations of the synaptic connections—in fact, random oscillations around values given by a learning (for example, Hebb's) rule. The consequences for the system performance of a dynamics constantly checking at random the set of memorized patterns is thus studied both analytically and numerically. We describe various nonequilibrium phase transitions whose nature depends on the properties of fluctuations. We find, in particular, that under rather general conditions locally stable mixture states do not occur, and pattern recognition and retrieval processes are substantially improved for some classes of synaptic fluctuations.

KEY WORDS: Neural network; synaptic noise; stochastic Hopfield model.

1. INTRODUCTION, AND DEFINITION OF MODEL

The Hopfield neural network[1] was recently re-formulated as a kinetic stochastic system in which synapse intensities change with time, namely, they have their own local dynamics competing with neuronal activity.[2] It was argued that such a competition may occur in biological systems. For example, biological neurons typically connect each other by more than one synapse, each having a different nature, therefore transmitting the action potential at different speed,[3] and emission of neurotransmitters and related mechanisms have an essential random component.[4, 5] These features of biological systems induce apparently-noisy behavior of synaptic

[1] Instituto Carlos I de Física Teórica y Computacional, and Departamento de Electromagnetismo y Física de la Materia, Universidad de Granada, E-18071 Granada, Spain.
[2] Present address: Institute for Nonlinear Studies, University of California, San Diego, La Jolla, California 92093-0402.

0022-4715/99/0300-0837$16.00/0

patterns. The observed variability of response to the same stimulus of a given neuron[6] also suggests random synaptic variations with time. Such a possibility is, in fact, appealing, as a growing literature which reports on noisy, unreliable behavior of individual biological synapses (see, for instance, refs. 7–14) coexists with the spreading belief (see refs. 7, 9, 12, 13, and 15–18, for instance) that "noise" is likely to be at the origin of the observed robustness and high processing power of biological networks. In summary, various recent observations support that neuron updates are slow and they occur under the action of a rapidly varying, apparently noisy stimulus from the synapses.

As a step further towards incorporating these features and better understanding the consequences of synaptic variations on the network behavior, we studied in some detail a set of N binary *neurons* with configurations $\mathbf{s} = \{s_{\mathbf{x}} = \pm 1;\ \mathbf{x} = 1,..., N\}$ which evolve by stochastic equations,

$$\partial_t P_t(\mathbf{s}) = \sum_{\mathbf{x}} [\, w(\mathbf{s}^{\mathbf{x}}; \mathbf{x})\, P_t(\mathbf{s}^{\mathbf{x}}) - w(\mathbf{s}; \mathbf{x})\, P_t(\mathbf{s})\,] \tag{1}$$

where the transition probability per unit time (*rate*) is a superposition, namely,

$$w(\mathbf{s}; \mathbf{x}) = \int d\mathbf{J}\, f(\mathbf{J})\, \varphi[\, 2T^{-1} s_{\mathbf{x}} h_{\mathbf{x}}(\mathbf{s}, \mathbf{J})\,] \tag{2}$$

Here $\mathbf{s}^{\mathbf{x}}$ is the configuration obtained from $\mathbf{s}$ after the change $s_{\mathbf{x}} \to -s_{\mathbf{x}}$, $\mathbf{J} = \{J_{xy} \in \Re\}$ stands for synapse configurations, and T is the temperature of the heat bath involved; $h_{\mathbf{x}}(\mathbf{s}, \mathbf{J}) = \sum_{\mathbf{y} \neq \mathbf{x}} J_{xy} s_{\mathbf{y}} - \theta_{\mathbf{x}}$ is a local field with $\theta_{\mathbf{x}}$ the threshold energy needed to activate the neuron at $\mathbf{x}$ (for simplicity, we assume $\theta_{\mathbf{x}} = 0\ \forall \mathbf{x}$ hereafter). The function φ stands for the elementary dynamic rate, which—for simplicity—we assume satisfies detailed balance, $\varphi(X) = \varphi(-X) \exp(-X)$, and $\varphi(0) = 1$ and $\lim_{X \to +\infty} \varphi(X) = 0$; we consider explicitly

$$\varphi(X) = \begin{cases} e^{-X/2}, & \text{rule } V \\ 2(1 + e^{X})^{-1}, & \text{rule } K \\ \min\{1, e^{-X}\}, & \text{rule } M \end{cases} \tag{3}$$

The interpretation of the above[2] is that, once a learning (*plasticity*) process is completed, the neuron subsystem varies on a (coarse) time scale t, whilst the synapse subsystem also varies but on a finer time scale, e.g., $\tau = tp^{-1}$ for small p. For $p \to 0$, and $\tau \to \infty$, synapses change very fast compared to neuron changes, and one may consider the couplings J_{xy} as random

variables of distribution $f(\mathbf{J})$. The result is the effective rate for transitions $s_{\mathbf{x}} \to -s_{\mathbf{x}}$ given in (2). This indicates that the evolution of $\mathbf{s}$ is by a competition of different canonical mechanisms, $\varphi[2T^{-1}s_{\mathbf{x}}h_{\mathbf{x}}(\mathbf{s}, \mathbf{J})]$, each corresponding to a different local field $h_{\mathbf{x}}(\mathbf{s}, \mathbf{J})$, such that the superposition (2) will not satisfy detailed balance in general. Therefore, the system evolves asymptotically towards a *nonequilibrium* steady state which is expected to exhibit a strong dependence on both $f(\mathbf{J})$ and $\varphi(X)$, i.e., on the fluctuating properties of the synapses.

The consequences of the competition (2) were studied explicitly in ref. 2 for

$$f(\mathbf{J}) = \prod_{\substack{\mathbf{x},\,\mathbf{y} \\ \mathbf{x} \neq \mathbf{y}}} \sum_{\mu=1}^{P} a_\mu \delta(J_{xy} - \eta_{xy}^{\mu}) \tag{4}$$

$\sum_{\mu=1}^{P} a_\mu = 1$. The factorization in this function implies that fluctuations at different synapses are not correlated with each other (though one may imagine a kind of stationary waves propagating in the network). Assuming that the system has previously stored P patterns, $\boldsymbol{\xi}^\mu \equiv \{\xi_{\mathbf{x}}^\mu = \pm 1\}$ with $\mu = 1,..., P$, an interesting choice is $\eta_{xy}^{\mu} \propto \xi_{\mathbf{x}}^{\mu}\xi_{\mathbf{y}}^{\mu}$, i.e., each synapse intensity is associated to one of the elements of a memorized pattern. This case admits a quasi-canonical representation in terms of an effective Hamiltonian,[19] and some exact results may then be obtained. In spite of such simplicity, the resulting behavior is rather involved for some rates φ. For the cases in ref. 2, however, fluctuations simply modify the temperature T, which changes to some "effective" (larger) value, as in the presence of some excess noise. Consequently, the value α_C, for the ratio $\alpha \equiv P/N$ below which there is efficient associative memory (slightly) decreases, and the region of the phase diagram where the occurrence of mixture ("spin-glass") states hampers memory is notably reduced, and it does not occur at zero temperature above a certain value for α.

The only motivation for the choice (4) was simplicity; for example, the model in ref. 2 can be solved exactly. In this paper we try to understand better the influence of synapse dynamics on the performance of neural-network models by studying synapse fluctuations that can be spatially correlated. In particular, we report on the emergent behavior following from (1)–(3) for

$$f(\mathbf{J}) = \sum_{\mu=1}^{P} a_\mu \prod_{\substack{\mathbf{x},\,\mathbf{y} \\ \mathbf{x} \neq \mathbf{y}}} \delta(J_{xy} - \eta_{xy}^{\mu}) \tag{5}$$

$\sum_{\mu=1}^{P} a_\mu = 1$. The choice $\eta_{xy}^{\mu} \propto \xi_{\mathbf{x}}^{\mu}\xi_{\mathbf{y}}^{\mu}$ then implies that each pattern $\boldsymbol{\xi}^\mu$ contributes with some probability to the configuration $\mathbf{J}$; therefore, in general,

correlations between the fluctuations at different synapses exist in this case due to the spatial correlations in ξ^{μ}. In order to have a well-known reference, we shall assume that the random variations with time of each intensity J_{xy} are such that its average, $\overline{J_{xy}}$, along the characteristic time interval for neuronal activity has the value corresponding to a given learning rule. For example, assuming $\eta_{xy}^{\mu} = (Na_{\mu})^{-1} \xi_{\mathbf{x}}^{\mu} \xi_{\mathbf{y}}^{\mu}$, we have

$$\overline{J_{xy}} \equiv \int d\mathbf{J}\, f(\mathbf{J})\, J_{xy} = \frac{1}{N} \sum_{\mu=1}^{P} \xi_{\mathbf{x}}^{\mu} \xi_{\mathbf{y}}^{\mu} \tag{6}$$

i.e., fluctuations are around mean values corresponding to Hebb's learning rule.[20] It is also to be noted at this point that our analytical results in the following concern the *thermodynamic limit* or infinite network, $N \to \infty$, and that explicit behavior is only reported for finite P; however, we believe, and present some evidence that our conclusions most likely hold well for arbitrarily large P, i.e., they belong to the asymptotic regime for $P \to \infty$. A preliminary account of some of our results here (mostly the ones obtained numerically) has been published elsewhere.[21]

2. CONTINUOUS PHASE TRANSITIONS

The mean activity follows from (1) after using (2) and (5):

$$\partial_t \langle s_{\mathbf{x}} \rangle = -2 \left\langle s_{\mathbf{x}} \sum_{\mu=1}^{P} a_{\mu} \mathscr{A}_{\mu,\mathbf{x}}^{+}(\mathbf{s}) \right\rangle - 2 \left\langle \sum_{\mu=1}^{P} a_{\mu} \mathscr{A}_{\mu,\mathbf{x}}^{-}(\mathbf{s}) \right\rangle \tag{7}$$

where $\mathscr{A}_{\mu,\mathbf{x}}^{\pm}(\mathbf{s}) = \frac{1}{2}\{\varphi[2T^{-1} \sum_{\mathbf{y}} \eta_{xy}^{\mu} s_{\mathbf{y}}] \pm \varphi[-2T^{-1} \sum_{\mathbf{y}} \eta_{xy}^{\mu} s_{\mathbf{y}}]\}$. The field $h_{\mathbf{x}}(\mathbf{s}, \mathbf{J}) = \sum_{\mathbf{y} \neq \mathbf{x}} J_{xy} s_{\mathbf{y}}$ involves interaction between a given neuron and the rest. A simple ansatz consistent with such *long-range interactions* is $s_{\mathbf{x}} = \langle s_{\mathbf{x}} \rangle$. (The analytical consequences of this agree with the results from Monte Carlo simulations within statistical errors; see Section 6.) It follows the stationary solution

$$\langle s_{\mathbf{x}} \rangle = \sum_{\mu=1}^{P} a_{\mu} [\varphi(-\zeta_x^{\mu}) - \varphi(\zeta_x^{\mu})] \left\{ \sum_{\mu=1}^{P} a_{\mu} [\varphi(-\zeta_x^{\mu}) + \varphi(\zeta_x^{\mu})] \right\}^{-1} \tag{8}$$

where $\zeta_x^{\mu} \equiv 2T^{-1} \sum_{\mathbf{y}} \eta_{xy}^{\mu} \langle s_{\mathbf{y}} \rangle$. As this holds for $\langle s_{\mathbf{x}} \rangle = 0 \ \forall \mathbf{x}$, nontrivial solutions corresponding to continuous phase transitions may be obtained by expanding (8) in powers of $\langle s_{\mathbf{x}} \rangle$, which leads to first order to

$$\langle s_{\mathbf{x}} \rangle \approx \tfrac{1}{2} \sum_{\mu} a_{\mu} \zeta_x^{\mu} \tag{9}$$

That is, $\langle s_{\mathbf{x}} \rangle \neq 0$ (only) below a critical temperature, T_c, which is the solution of $\det\{T^{-1} \sum_\mu a_\mu \eta^\mu_{xy} - \delta_{xy}\} = 0$. In spite of some similarities with the equilibrium transition of second order, this has a nonequilibrium nature[19] which reflects, for instance, in the fact that T_c depends on the choice for η^μ_{xy}, i.e., on $f(\mathbf{J})$ and, consequently, on the (effective) rate (2). It is true that, in the present case, T_c is independent of φ; however, the validity of (9) breaks down as T is lowered so that, in general, the stationary states below T_c depend also on φ. More explicitly, they exhibit a dependence on the asymptotic properties of $\varphi(X)$ as $X \to \pm\infty$; in fact, due to detailed balance, only the value of $\lim_{X \to -\infty} \varphi(X) = \rho \exp(-\Delta X)$—where $\rho = 1$, $\Delta = 1/2$ for rule V; $\rho = 2$, $\Delta = 0$ for rule K; and $\rho = 1$, $\Delta = 0$ for rule M—matters at sufficiently low T.

As a first example, consider $\eta^\mu_{xy} = N^{-1}\eta^\mu$, i.e., one has $J_{xy} = N^{-1}\eta^\mu$, $\forall \mathbf{x}, \mathbf{y}$ with probability a_μ. Equation (9) then predicts a transition from paramagnetic- to ferromagnetic-like states at $T_c = \sum_\mu a_\mu \eta^\mu$. As $T \to 0$, one has from (8) that $\langle s_{\mathbf{x}} \rangle = \pm \sum_\mu a_\mu \operatorname{sign}(\eta^\mu)$ for $\sum_\mu a_\mu \operatorname{sign}(\eta^\mu) > 0$ and $\langle s_{\mathbf{x}} \rangle = 0$ otherwise for both rules K and M ($\Delta = 0$), and $\langle s_{\mathbf{x}} \rangle = \pm 1$ for $\operatorname{sign}(\eta^\alpha) > 0$ and $\langle s_{\mathbf{x}} \rangle = 0$ otherwise for rule V ($\Delta \neq 0$). The index α stands for the pattern for which $|\eta^\alpha| = \max_\mu |\eta^\mu|$.

As a further example, consider $\eta^\mu_{xy} = \lambda_\mu \xi^\mu_{\mathbf{x}} \xi^\mu_{\mathbf{y}}$ with $\lambda_\mu > 0$. The interest is then on the conditions for which (7) has stationary solutions whose overlap with a given pattern ξ^μ, defined as

$$m_\mu(\mathbf{s}) \equiv \frac{1}{N} \sum_{\mathbf{x}} \xi^\mu_{\mathbf{x}} s_{\mathbf{x}} \tag{10}$$

is nonzero. We obtain from (9) that such solutions occur when

$$\sum_\mu m_\mu \left(\delta_{\mu\nu} - T^{-1} \sum_{\mathbf{x}} a_\mu \lambda_\mu \xi^\mu_{\mathbf{x}} \xi^\nu_{\mathbf{y}} \right) = 0 \tag{11}$$

where m_μ stands hereafter for $m_\mu(\mathbf{s})$ with $s_{\mathbf{x}} = \langle s_{\mathbf{x}} \rangle \ \forall \mathbf{x}$.

Approaching analytically the properties of our system becomes simpler for *orthogonal* patterns. This names those patterns whose elements, $\xi^\mu_{\mathbf{x}}$, are either orthogonal to each other, namely, $N^{-1} \sum_{\mathbf{x}} \xi^\mu_{\mathbf{x}} \xi^\nu_{\mathbf{x}} = \delta_{\mu\nu}$, or else quasi-orthogonal, as when $\{\xi^\mu_{\mathbf{x}}\}$ is a set of $P \times N$ statistically-independent random variables, so that $N^{-1} \sum_{\mathbf{x}} \xi^\mu_{\mathbf{x}} \xi^\nu_{\mathbf{x}} \to \delta_{\mu\nu}$ as $N \to \infty$ (with finite P), which is the limit we consider for the analytical results hereafter. For orthogonal patterns, (11) implies $m_\mu \neq 0$ for $T < T_c$, where T_c is independent of the rate φ. More explicitly, a continuous phase transition occurs at $T_c = \max_\mu a_\mu$ if $\lambda_\mu = N^{-1}$ and $T_c = 1$ if $\lambda_\mu = (N a_\mu)^{-1}$. The latter case, which

corresponds to fluctuations around the Hebbian rule, is studied below. On the other hand, as $T \to 0$, one obtains for $\eta_{xy}^{\mu} = \lambda_{\mu} \xi_{\mathbf{x}}^{\mu} \xi_{\mathbf{y}}^{\mu}$, independently of the choice for λ_{μ}, that $m_{\mu} = \pm a_{\mu}$ for rules K and M, and $m_{\mu} = \delta_{\mu\varkappa} \operatorname{sign}(m_{\varkappa})$ $\forall \mu$ for rule V; $\varkappa$ stands for the pattern for which $|m_{\varkappa}| = \max_{\mu} |m_{\mu}|$. The fact that the behavior near the ground state depends qualitatively on (2) deserves analysis in subsequent sections.

3. FLUCTUATIONS AROUND HEBB'S RULE

Though the following restriction is not necessary to obtain our main result in this paper, we study here fluctuations around values determined by a given learning rule; in this section (and in Section 6) we consider explicitly the Hebbian case. This corresponds to the choice $\eta_{xy}^{\mu} = (N a_{\mu})^{-1} \xi_{\mathbf{x}}^{\mu} \xi_{\mathbf{y}}^{\mu}$, which induces fluctuations of mean (6), and

$$\sigma_{xy}^2(\boldsymbol{\xi}) = \overline{(J_{xy} - \overline{J_{xy}})^2} = \left(\frac{P}{N}\right)^2 - \frac{1}{N^2} \sum_{\mu,\, \nu} \xi_{\mathbf{x}}^{\mu} \xi_{\mathbf{y}}^{\mu} \xi_{\mathbf{x}}^{\nu} \xi_{\mathbf{y}}^{\nu} \tag{12}$$

where $\boldsymbol{\xi}$ stands for the set $\{\xi^{\mu};\ \mu = 1, \ldots, P\}$ of all memorized patterns. In this case, for $s_{\mathbf{x}} = \langle s_{\mathbf{x}} \rangle$ and *orthogonal patterns*, (1) transforms for (5) into

$$\partial_t m_{\mu} = -2 m_{\mu} \sum_{\nu=1}^{P} a_{\nu} \mathscr{B}_{\nu}^{+} - 2 a_{\mu} \mathscr{B}_{\mu}^{-} \tag{13}$$

where $\mathscr{B}_{\mu}^{\pm} = \frac{1}{2} \{ \varphi((2/a_{\mu} T)\, m_{\mu}) \pm \varphi(-(2/a_{\mu} T)\, m_{\mu}) \}$. The stationary solution is $\mathbf{m} = (m^1, \ldots, m^P)$ with

$$m_{\mu} = -a_{\mu} \mathscr{B}_{\mu}^{-} \left(\sum_{\nu=1}^{P} a_{\nu} \mathscr{B}_{\nu}^{+} \right)^{-1} \tag{14}$$

This admits the trivial solution $(0, 0, \ldots, 0)$, and solutions $(m^1, \ldots, m^n, 0, \ldots, 0)$ with $n \leqslant P$ and $1 \geqslant |m_{\mu}| \geqslant 0$ for $T < T_c = 1$. The stability of these solutions, which in general depends on φ, is studied in Section 4.

The property of associative memory relies on solutions with $n = 1$, i.e., the so-called Mattis or pure states;[22] for P stored patterns, ξ^{μ}, there are $2P$ Mattis states, namely, the elements of the two set ξ^{μ} and $-\xi^{\mu}$. The mixture or "spin-glass" solutions with $n > 1$ are $\mathbf{m} = m_n(1, \ldots, 1, -1, \ldots, -1, 0, \ldots, 0)$ for a_{μ} independent of μ, i.e., $a_{\mu} = P^{-1}$ so that all the stored patterns contribute the same to the synaptic intensities. These states are said to be symmetric if either the number, k, of 1s or else the number, s, of -1s, $n = k + s$, are zero, and asymmetric otherwise.

Explicit results generally depend on φ. For rule K, (14) is $m_\mu = a_\mu x_0(T)$ with $x_0 = \tanh(T^{-1}x_0)$, i.e., $m_\mu \propto a_\mu$ for given T. The behavior near $T_c = 1$ is

$$m_\mu \sim \pm\sqrt{3}\, a_\mu T_c (T_c - T)^{1/2}, \qquad T \to T_c^- \tag{15}$$

and $m_\mu = \pm a_\mu$ as $T \to 0$. For $a_\mu = P^{-1}$, m_μ for given T is either 0 or $\pm P^{-1} |x_0(T)|$, i.e., the overlap decreases as the number P of patterns increases.

For rule M, (14) is

$$|m_\mu| = \frac{a_\mu [1 - \exp(-2T^{-1} a_\mu^{-1} |m_\mu|)]}{\sum_{\nu=1}^{P} a_\nu [1 + \exp(-2T^{-1} a_\nu^{-1} |m_\nu|)]} \tag{16}$$

i.e., m_μ depends on a_μ and on the other $P-1$ overlaps, unlike for rule K. The low temperature behavior depends on the type of solution (m_1,..., m_n, 0,..., 0). For $n = P$ (all overlaps are nonzero), one has $|m_\mu| = a_\mu$ at $T = 0$, as for rule K; for $P - n$ (>0) zero overlaps, however, the other n nonzero overlaps at $T = 0$ are $|m_\mu| = a_\mu [1 + \sum_{\nu=n+1}^{P} a_\nu]^{-1}$. If the stored patterns are equiprobable, $a_\mu = P^{-1}$, m_μ is either 0 or $\pm |m_n|$ for any T, and it follows below $T_c = 1$ that

$$|m_n| = \begin{cases} (P-n)^{-1} T_c (T_c - T), & n < P \\ \sqrt{3}\, P^{-1} T_c (T_c - T)^{1/2}, & n = P \end{cases} \qquad \text{as} \quad T \to T_c^- \tag{17}$$

This transforms continuously into $|m_n| = (2P - n)^{-1}$, $n \leqslant P$, as $T \to 0$.

For rule V, (14) reads

$$m_\mu = a_\mu \sinh(T^{-1} a_\mu^{-1} m_\mu) \left[\sum_{\nu=1}^{P} a_\nu \cosh(T^{-1} a_\mu^{-1} m_\nu) \right]^{-1} \tag{18}$$

so that m_μ depends on a_μ and on the other $P-1$ overlaps, as in (16). At zero-T:

$$m_\mu = a_\mu \left(\sum_{\nu=1}^{n_\varkappa} a_\nu \right)^{-1} \operatorname{sign}(m_\mu)\, \delta_{\varkappa\mu} \tag{19}$$

$|m_\varkappa| = \max_\mu |m_\mu|$, where $n_\varkappa$ is the number of overlaps $|m_\mu| = |m_\varkappa|$. It follows $m_\mu = \operatorname{sign}(m_\mu)\, \delta_{\varkappa\mu}$ for $n_\varkappa = 1$, i.e., the system recovers without error at $T = 0$.

For $T > 0$, we studied the simplest case, i.e., $a_\mu = P^{-1}$ with $m_\mu = 0$, $\pm |m_n|$, where m_n depends on T, n, and P. Unlike for rules K and M, two

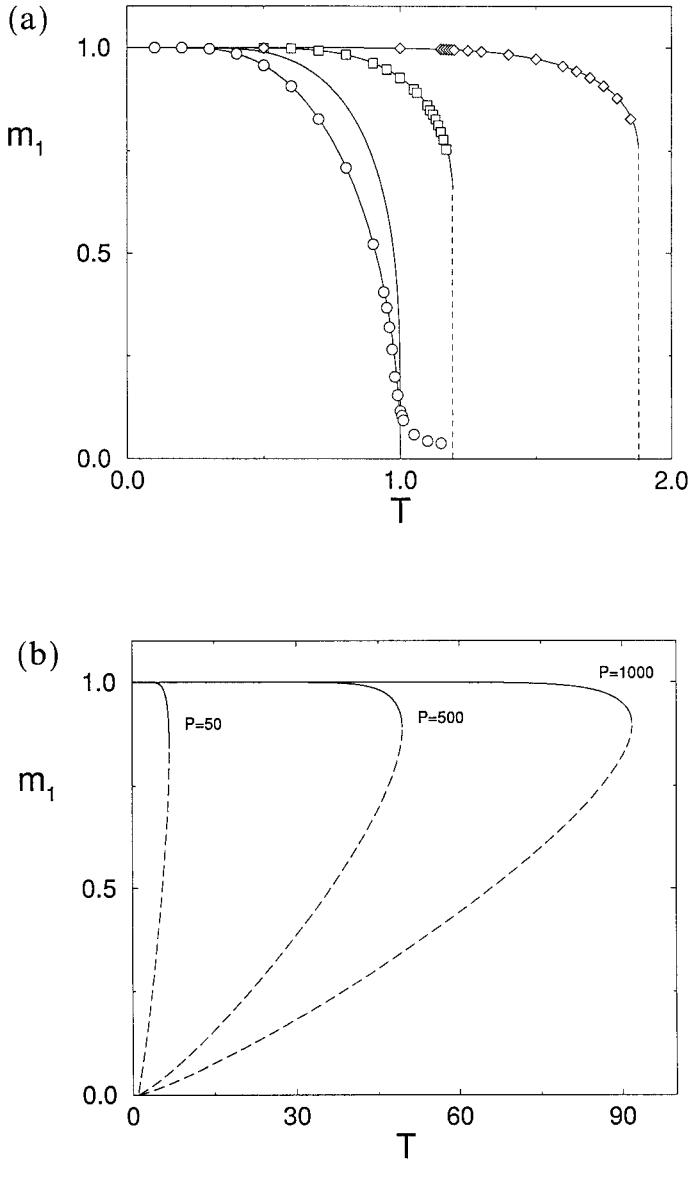

Fig. 1. The variation with P of stable solutions $m_n(T)$ for $n=1$ (pure, Mattis states) as obtained from (18), *rule V* (solid lines). (a) For $P=1$, 3, 5, and 10, from left to right. Monte Carlo data for $N=3600$ and $P=1$ ($\bigcirc$), 5 ($\square$), and 10 ($\diamond$) are also shown. The dashed lines correspond to the discontinuity that occurs at $\tilde{T}(n, P)$ for any $P>3n$. (b) The same for $P=50$, 500, and 1000, which illustrates the tendency shown for large P. The dashed lines here correspond to unstable solutions which connect $\tilde{T}(1, P>3)$ with $T=1$.

different types of mixture may occur: For $n > \frac{1}{3}P$, one has $m_n = 0$ for $T > T_c = 1$, and $|m_n| = \sqrt{6}[P(3n-P)]^{-1/2} T_c (T_c - T)^{1/2}$ as $T \to T_c^-$. For $n \leqslant \frac{1}{3}P$, however, m_n behaves discontinuously at $\tilde{T}(n, P) \equiv \tilde{m}_n P \theta_n^{-1}$, where θ_n is the solution of

$$n\theta_n + (P-n)(\theta_n \cosh \theta_n - \sinh \theta_n) - n \sinh \theta_n \cosh \theta_n = 0 \tag{20}$$

and

$$\tilde{m}_n = \sinh \theta_n (n \cosh \theta_n + P - n)^{-1} \tag{21}$$

is m_n for $T = \tilde{T}(n, P)$; $\tilde{T}(n, P < 3n) = T_c$. The fact that this transition is of first order, in general, allows for large overlaps $\tilde{m}_n$ just below $\tilde{T}$, which corresponds to a good performance of the system. In any case, $|m_n| = n^{-1}$ as $T \to 0$.

This behavior for rule V is illustrated in Figs. 1 to 3 for the Mattis case. The graphs indicate, in particular, the existence of a *nonequilibrium tricritical point* at $P = 3$. In fact, the solutions (14) correspond, in general, to a saddle point with a number of instability directions, the details depending on the function $\varphi(X)$. It follows that, for rule V, only the Mattis

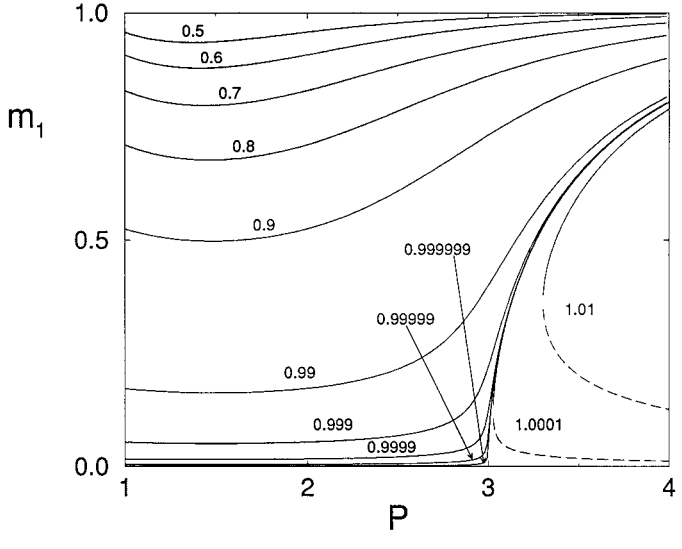

Fig. 2. The isotherms $m_n = m_n(P)$ for $n = 1$ and *rule V*, for indicated values of T, showing a (nonequilibrium) tricritical point. The dashed lines represent unstable solutions for $P > 3$ when $T < \tilde{T}(1, P)$. The solid lines represent the stable, continuous behavior for any P if $T < T_c = 1$.

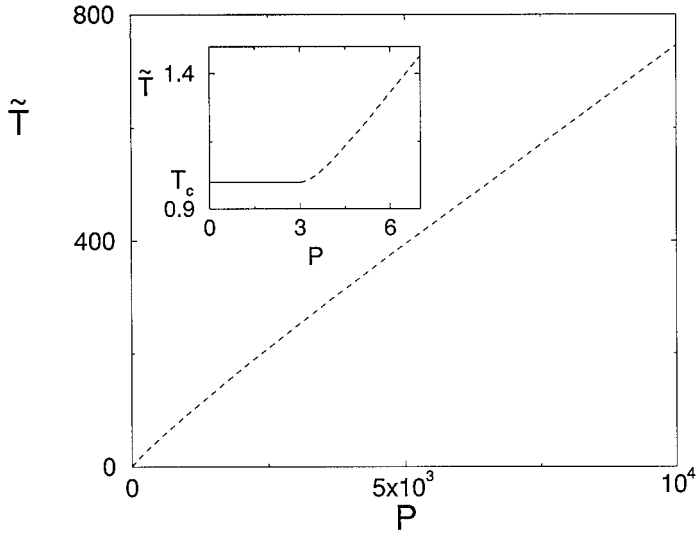

Fig. 3. Phase diagram for $n=1$ and *rule V*, as implied by (18), indicating $\tilde{T}(1, P)$ for small (inset) and large (main graph) P; the latter—showing $\tilde{T}(1, P)$ increasing less than linearly for $3 \leqslant P \leqslant 10^4$—suggests good behavior as P is increased. The graphs indicate (nonequilibrium) phase transitions of first (dashed lines) and second (solid line in the inset) order.

states ($n=1$) are locally stable, while local stability holds only for mixture states with $n=P$ if the rule is either K or M; this interesting result is worked out explicitly in the next section.

4. STABILITY, AND FIRST-ORDER PHASE TRANSITIONS

The (local) stability of solutions of (13), $m_{\mu,0}$, may be studied by linearizing:

$$\partial_t n^\mu = \sum_{\nu=1}^{P} \mathcal{Q}_{\mu\nu} n^\nu + \mathcal{O}(\mathbf{n}^2) \tag{22}$$

where $\mathbf{n}=(n^1,..., n^P)$ with $n^\mu \equiv m_\mu - m_{\mu,0}\ \forall \mu$ (see ref. 23, for instance). That is, the local stability of $\mathbf{m}=\mathbf{m}_0$ corresponds to the one of $\mathbf{n}=\mathbf{0}$, which requires that the eigenvalues of the matrix $\mathcal{Q}=(\mathcal{Q}_{\mu\nu})$ are negative. A first conclusion is that the stability of (14) depends, even qualitatively on $\varphi(X)$; see ref. 13.

For rule K,

$$\mathcal{Q}_{\mu\nu} = \left\{ \frac{2T^{-1}}{\cosh^2(T^{-1}a_\mu^{-1}m_\mu)} - 2 \right\} \delta_{\mu\nu} \tag{23}$$

where m_μ is given in (14), whose eigenvalues are

$$\tilde{\lambda}_\mu = \frac{2T^{-1}}{\cosh^2(T^{-1}a_\mu^{-1}m_\mu)} - 2 \quad \forall\mu \tag{24}$$

For $T < T_c = 1$, $\tilde{\lambda}_\mu < 0$ for $m_\mu \neq 0$ and $\tilde{\lambda}_\mu > 0$ for $m_\mu = 0$. Therefore, $(m_1,..., m_n, 0,..., 0)$ is a saddle point with $P-n$ instability directions, so that any mixture with $n < P$—in particular, the Mattis states $(n=1)$—is unstable; local stability only holds for mixtures with $n = P$, corresponding to nonzero overlaps with the P patterns. In other words, the steady state does not show associative memory when the case (5) of the model is implemented with rule K.

For rule M,

$$\mathcal{Q}_{\mu\nu} = 2T^{-1}\,|m_\mu|\,\Xi_\nu + \delta_{\mu\nu}\left\{[2T^{-1}\Xi_\nu] - \sum_{\alpha=1}^{P} a_\alpha(1+\Xi_\alpha)\right\} \tag{25}$$

where $\Xi_\nu \equiv \exp(-2T^{-1}\,|m_\nu|\,a_\nu^{-1})$ and $|m_\mu|$ is given in (16), which can hardly be diagonalized, in general. For $a_\mu = P^{-1}\ \forall\mu$, $T < T_c$, and mixtures with $n \leqslant P$ nonzero overlaps, one finds the eigenvalues

$$\begin{aligned}
\tilde{\lambda}_1 &= \frac{2}{T}(n\,|m_n|+1)\,e^{-2T^{-1}P\,|m_n|} + \frac{n}{P}(1-e^{-2T^{-1}P\,|m_n|}) - 2 \\
\tilde{\lambda}_2 &= \frac{2}{T}\,e^{-2T^{-1}P\,|m_n|} + \frac{n}{P}(1-e^{-2T^{-1}P\,|m_n|}) - 2 \\
\tilde{\lambda}_3 &= \frac{2}{T} + \frac{n}{P}(1-e^{-2T^{-1}P\,|m_n|}) - 2
\end{aligned} \tag{26}$$

where m_n is solution of (16); $\tilde{\lambda}_2$ and $\tilde{\lambda}_3$ have multiplicity $(n-1)$ and $(P-n)$, respectively. $\tilde{\lambda}_3 > 0$ so that mixtures (and Mattis states) with $n < P$ are unstable; for $n = P$, $\tilde{\lambda}_3$ does not occur, and $0 > \tilde{\lambda}_1$, $\tilde{\lambda}_2$, so that local stability holds.

For rule V,

$$\mathcal{Q}_{\mu\nu} = \left\{T^{-1}\Xi_\mu^{\mathrm{C}} - \sum_{\alpha=1}^{P} a_\alpha \Xi_\alpha^{\mathrm{C}}\right\}\delta_{\mu\nu} - T^{-1}m_\mu \Xi_\nu^{\mathrm{S}} \tag{27}$$

with $\Xi_\nu^{[\mathrm{S}]\{\mathrm{C}\}} = 2[\sinh]\{\cosh\}(m_\nu/a_\nu T)$, where m_μ is solution of (18). If $a_\mu = P^{-1}$, one may diagonalize $\mathcal{Q}$ for both symmetric mixtures ($n \leqslant P$ non-

zero overlaps m_n) and asymmetric mixtures (k overlaps $+m_n > 0$, and $n-k$ overlaps $-m_n$). The resulting eigenvalues are

$$\tilde{\lambda}_1 = -\frac{2}{P}\left[P - n + (n - T^{-1}P)\cosh(T^{-1}Pm_n) + nT^{-1}Pm_n \sinh(T^{-1}Pm_n)\right]$$

$$\tilde{\lambda}_2 = -\frac{2}{P}\left[P - n + (n - T^{-1}P)\cosh(T^{-1}Pm_n)\right] \tag{28}$$

$$\tilde{\lambda}_3 = -\frac{2}{P}\left[P(1 - T^{-1}) - n + n\cosh(T^{-1}Pm_n)\right]$$

where m_n is solution of (18), with multiplicity one, $(n-1)$ and $(P-n)$, respectively. One obtains $\tilde{\lambda}_2 > 0$, so that mixtures with $n > 1$ ($n = P$, in particular) are unstable; however, $\tilde{\lambda}_2$ does not occur when diagonalizing $\mathcal{Q}$, and both $\tilde{\lambda}_1$ and $\tilde{\lambda}_3$ are negative, so that the Mattis states ($n = 1$) are stable both for a continuous phase transition at $\tilde{T}(1,\ P < 3) = T_c = 1$ and for a discontinuous phase transition at $\tilde{T}(1,\ P \geqslant 3)$; see Section 3. Therefore, the system exhibits, at least locally, associative memory.

The resulting phase diagram for $n = 1$ and rule V is in Fig. 3, and Figs. 1 and 2 illustrate the nature of the solutions. Figure 4 depicts the variation

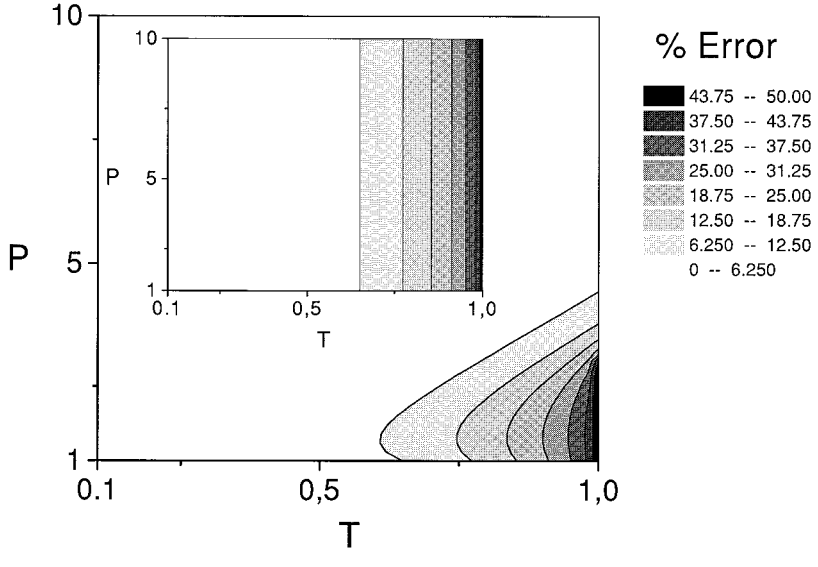

Fig. 4. (a) The percentage of error, as measured by $\frac{1}{2}(1 - m_1)$, as a function of P and T, during a typical retrieval process in our model with *rule V* (main graph) and in the corresponding Hopfield case (inset). The darkness is proportional to the error, as indicated.

with T and P of the percentage of error during retrieval processes, and a comparison with the corresponding Hopfield case. A definite conclusion here is that synaptic noise of the sort considered here significantly improves the system performance as a device for associative memory.

Our results above concern finite P, and the limit $N \to \infty$ (which is either explicitly taken in some examples or implicitly assumed when one uses a mean-field condition). In practice, better performance generally requires larger and larger values of P/N, so that studying the behavior for large P is interesting. (In Section 6 we numerically study finite values for both P/N and N.) We have concluded in Section 3 that the relevant phase transition occurs at temperature $\tilde{T}(n, P) = \tilde{m}_n P \theta_n^{-1}$, where θ_n and $\tilde{m}_n$ are defined in (20) and (21), respectively. The variation with P of the latter, which represents the value of the overlap $m_n(T)$ for $T = \tilde{T}(n, P)$, is depicted in Fig. 5 for the Mattis case $n = 1$; this illustrates the tendency $\tilde{m}_n \to 1$ as $P \to \infty$. The behavior of θ_n for large P is illustrated in Fig. 6; the situation here seems to confirm our belief that most analytical results in this paper belong to the asymptotic regime for $P \to \infty$. In fact, one may notice that Eqs. (2) and (5) imply that a relevant parameter in our case is P/T rather than P/N.

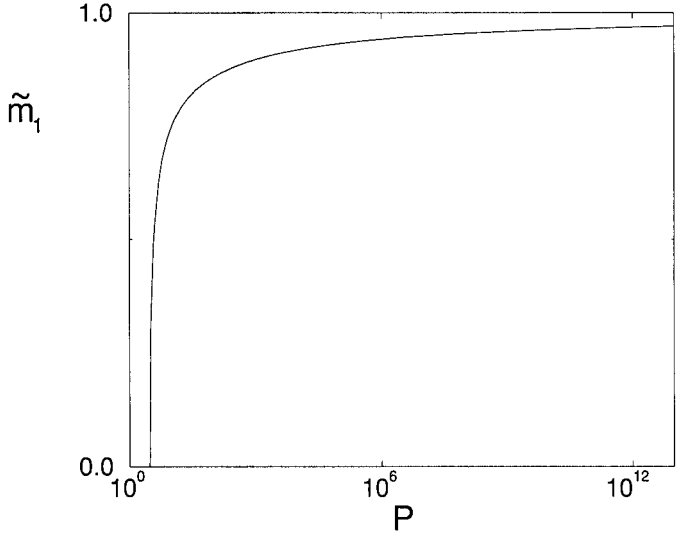

Fig. 5. Semilogarithmic plot of the variation with P of the critical value (at T_c) of $\tilde{m}_n$ for $n = 1$, as defined in (21), corresponding to the characteristic overlap for stable Mattis states for *rule V*. This shows that $\tilde{m}_1$ becomes small (only) for very small P, and $\tilde{m}_1 \to 1$ as $P \to \infty$.

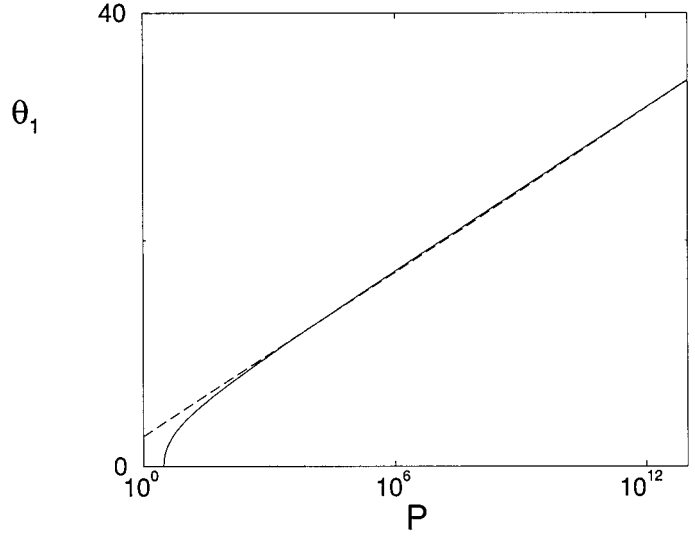

Fig. 6. Semilogarithmic plot of the variation with P of θ_n, as defined in (20), for the Mattis case, $n=1$ (solid curve). The dashed line is a rough linear fit to θ_1 for $P \in [10^4, 10^{13}]$ giving $\theta_1 \simeq 2.663 + 1.051 \ln P$.

5. ASYMMETRIC SYNAPSIS

The theory we have just described for fluctuations around the Hebbian rule may be generalized to include other learning rules and, in particular, those that allow for asymmetric synapsis. As an illustration, we consider next distributions $f(\mathbf{J})$ as in (5) with $\eta^{\mu}_{xy} \neq \eta^{\mu}_{yx}$. A relatively general case of this corresponds to $\eta^{\mu}_{xy} = (a_\mu N)^{-1} (A\xi^{\mu}_{\mathbf{x}}\xi^{\mu}_{\mathbf{y}} + B\xi^{\mu}_{\mathbf{x}} + C\xi^{\mu}_{\mathbf{y}} + D)$, which induces mean values:

$$\bar{J}_{x,y} = \frac{1}{N} \sum_{\mu=1}^{P} (A\xi^{\mu}_{\mathbf{x}}\xi^{\mu}_{\mathbf{y}} + B\xi^{\mu}_{\mathbf{x}} + C\xi^{\mu}_{\mathbf{y}} + D) \tag{29}$$

Parameters B and C determine the grade of asymmetry. One obtains from (7) that

$$\partial_t \langle s_{\mathbf{x}} \rangle = -2 \left\langle s_{\mathbf{x}} \sum_{\mu} a_\mu \mathscr{A}_\mu(\mathbf{s}) \right\rangle - 2 \left\langle \sum_{\mu} a_\mu [\xi^{\mu}_{\mathbf{x}} + \mathscr{C}_\mu(\mathbf{s})] \, \mathscr{B}_\mu(\mathbf{s}) \right\rangle \tag{30}$$

where

$$\begin{aligned}
\mathscr{A}_\mu(\mathbf{s}) &= \tfrac{1}{2}\{[1-\mathscr{C}_\mu(\mathbf{s})]\,\varphi(X_\mu^+(\mathbf{s})) + [1+\mathscr{C}_\mu(\mathbf{s})]\,\varphi(X_\mu^-(\mathbf{s}))\} \\
\mathscr{B}_\mu(\mathbf{s}) &= \tfrac{1}{2}\{\varphi(X_\mu^+(\mathbf{s})) - \varphi(X_\mu^-(\mathbf{s}))\} \\
\mathscr{C}_\mu(\mathbf{s}) &= [\,Cm_\mu(\mathbf{s}) + Dm(\mathbf{s})][\,Am_\mu(\mathbf{s}) + Bm(\mathbf{s})]^{-1}
\end{aligned} \tag{31}$$

with $X_\mu^\pm(\mathbf{s}) \equiv \pm(2/a_\mu T)[(A \pm C)\, m_\mu(\mathbf{s}) + (B \pm D)\, m(\mathbf{s})]$. The overlap $m_\mu(\mathbf{s})$ has been defined in (23), and $m(\mathbf{s}) \equiv N^{-1}\sum_{\mathbf{x}} s_{\mathbf{x}}$ is the mean activity. Equation (30) leads under the mean-field condition to a set of coupled equations that, assuming that the patterns are orthogonal (see Section 2), imply to first order that

$$\partial_t \mathbf{M} = -2\mathbf{M}\sum_\mu a_\mu \mathscr{A}_\mu - 2\mathbf{N} \tag{32}$$

where $\mathbf{M}$ and $\mathbf{N}$ are $(P+1)$-dimensional vectors of components $M_0 = m$, $N_0 = \sum_\mu a_\mu \mathscr{C}_\mu \mathscr{B}_\mu$, $M_\mu = m_\mu$, and $N_\mu = a_\mu \mathscr{B}_\mu$, and m, m_μ, $\mathscr{A}_\mu$, $\mathscr{B}_\mu$ and $\mathscr{C}_\mu$ stand for $m(\mathbf{s})$, $m_\mu(\mathbf{s})$, $\mathscr{A}_\mu(\mathbf{s})$, $\mathscr{B}_\mu(\mathbf{s})$ and $\mathscr{C}_\mu(\mathbf{s})$, respectively, with $s_{\mathbf{x}}$ replaced by $\langle s_{\mathbf{x}} \rangle$.

The stability of (32) may be studied as in Section 4. After linearization, the matrix whose eigenvalues determine local stability follows as

$$\mathscr{L}_{ij} = -2\sum_k a_k\{\delta_{ij}\mathscr{A}_k + M_i\mathscr{D}_{kj}^+ + \delta_{ik}\mathscr{D}_{kj}^- + (\delta_{ik} - M_i)(\mathscr{C}_k\mathscr{D}_{kj}^- + \mathscr{B}_k\mathscr{E}_{kj})\} \tag{33}$$

where

$$\begin{aligned}
\mathscr{D}_{ij}^\pm = \frac{1}{Ta_i}\{&\Psi(X_i^+)[(A+C)\,\delta_{ij} + (B+D)\,\delta_{0j}] \\
&\pm \Psi(X_i^-)\{(C-A)\,\delta_{ij} + (D-B)\,\delta_{0j}\}\}
\end{aligned} \tag{34}$$

and

$$\mathscr{E}_{ij} = (AD - BC)(M_i\delta_{0j} - M_0\delta_{ij})(AM_i + BM_0)^{-2} \tag{35}$$

with $\Psi(X_i^\pm) \equiv [\partial\varphi(X)/\partial X]_{X = X_i^\pm}$. The stationary behavior of m_μ and m as a function of T and P may then be obtained numerically from (32) and (33). A key result is that, as for the symmetric case, the asymmetric network exhibits stable Mattis states for rule V, but not for rules K or M. Furthermore, one obtains that the properties of the associative memory which occurs for rule V strongly depend on the value for the asymmetric

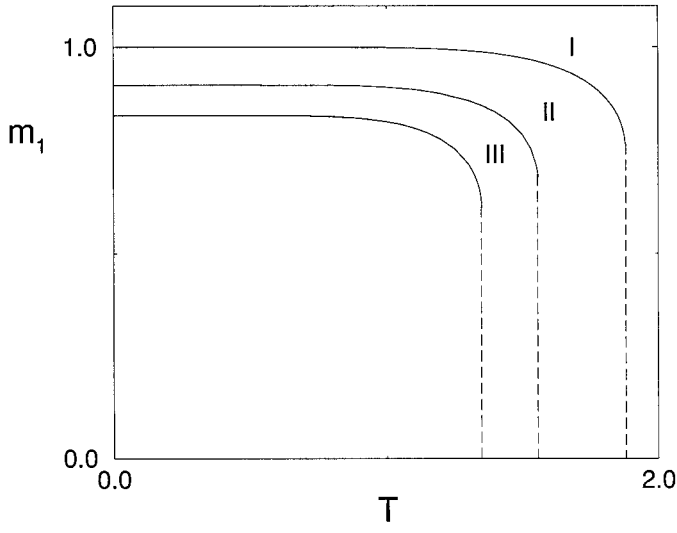

Fig. 7. This illustrates the nature of stable Mattis states, for which only the overlap (m_1) with one of the patterns is nonzero, as in Fig. 1(a), but for asymmetric synapses. Different graphs here correspond to the stationary solution of (32) as a function of T for $P=10$ and different choices of the asymmetric parameters, namely, $A=1$, $D=0$, and (from right to left) $B=C=0$ (I), $C=-B=0.1$ (II), and $B=\frac{1}{2}C=0.1$ (III).

parameters in (29). It follows, in particular, that asymmetric rules such that $A, B\neq 0$ and $C=D=0$ imply $\mathscr{C}_\mu=0$, which reduces (32) to (13) for orthogonal patterns, i.e., this situations is equivalent to considering fluctuations around the Hebbian rule. For any other choice, the resulting retrieval processes are quite varied. Figure 7 illustrates the nature of the Mattis states for different choices of the asymmetric parameters; corresponding results for fluctuations around the Hebbian rule are depicted in Fig. 1(a). Note that, as for symmetric rules, the transitions are discontinuous here.

6. SOME MONTE CARLO RESULTS

We have also simulated in the computer the stationary regime of our model using the Monte Carlo method. Our simulations concern N binary neurons, where N is between 400 and 3600, and $P=10$ memorized patterns generated at random. Typically, the system starts with a random initial configuration, and evolves by *flips*, $s_x\to -s_x$, according to the transition probability (2). This is implemented by one of the *rules* in (3). In practice, the flips are performed by using one of the following rates:

$$\begin{aligned}\varpi_1 &= \min\{1,\, e^{(2P/T)(1/N - s_{\mathbf{x}}(1/P)\sum_\mu S_{\mathbf{x}}^\mu)}\},\\ \varpi_2 &= e^{-(P/T)(1+s_{\mathbf{x}}(1/P)\sum_\mu S_{\mathbf{x}}^\mu)})\\ \varpi_3 &= \frac{1}{P}\sum_\mu e^{-(P/T)(1+s_{\mathbf{x}}S_{\mathbf{x}}^\mu)}\end{aligned} \tag{36}$$

$S_{\mathbf{x}}^\mu \equiv \xi_{\mathbf{x}}^\mu m_\mu(\mathbf{s})$, after normalizing to unity. The choices ϖ_1 and ϖ_2 correspond to the Hopfield case with the Hebbian learning rule $J_{xy} = N^{-1}\sum_\mu \xi_{\mathbf{x}}^\mu \xi_{\mathbf{y}}^\mu$. ϖ_1 is for *rule M*, i.e., the Metropolis algorithm, $\varphi(\Delta) = \min\{1, e^{-\Delta/T}\}$, where Δ is the change of energy brought about by the attempted flip as given by $\mathscr{H}_{\mathbf{J}}(\mathbf{s}) = -\frac{1}{2}\sum_{x\neq y} J_{xy}s_{\mathbf{x}}s_{\mathbf{y}}$. The rate ϖ_2 is similar to ϖ_1 but using *rule V* instead of *M*. The rate ϖ_3 characterizes our model with (5) and *rule V*. That is, it corresponds to random fluctuations of the synaptic intensities around mean values given by the Hebbian rule, as in (6). In any case, the symmetry $J_{xy} = J_{yx}$ is involved.

As expected, the data for ϖ_3 fit quite well our analytical results above, which generally concern a mean-field condition, except for familiar finite-size effects. That is, the condition that we have often used in previous sections to simplify analytics holds for the model with long-range interactions, in which any two neurons are in fact interconnected. This result is illustrated in Fig. 1(a) for $N = 3600$.

Figure 8 depicts another interesting feature of the system. The noisy horizontal behavior is the familiar (Hopfield) one implied by ϖ_1. That is, starting from any random initial state, $\mathbf{s}_0$, there is a rapid evolution (not visible on the scale of this figure) in which the overlap with one of the P memorized patterns becomes relatively large (around 0.7 in this simulation) while the others (of which only one case is shown) decay to very near zero. The situation remains stationary except for the thermal noise which is added to the signal; increasing T (equal to 0.8 in this simulation) would finally impede associative memory. For comparison purposes, Fig. 8 also illustrates the behavior for ϖ_2, i.e., the Hopfield case but a different choice for the elemtary rate $\varphi(\Delta)$. The retrieval process is then slower but more robust against thermal noise. Robustness here is a consequence of the fact that $e^{-\Delta/2T}$ favors low "energy" states more than the Metropolis algorithm. As illustrated in the figure, the performance of the retrieval process is further improved if the evolution proceeds according to ϖ_3, namely, in the presence of synaptic fluctuations such as those in (5). That is, although the convergence to the desired results is slower for ϖ_3 than for ϖ_1—but not than for ϖ_2, which corresponds to the same function $\varphi(\Delta)$—both the evolution and the stationary state are very robust, and the retrieval error is negligeable for these parameter values. The same qualitative behavior is observed varying N, P and T within wide ranges. It should be remarked

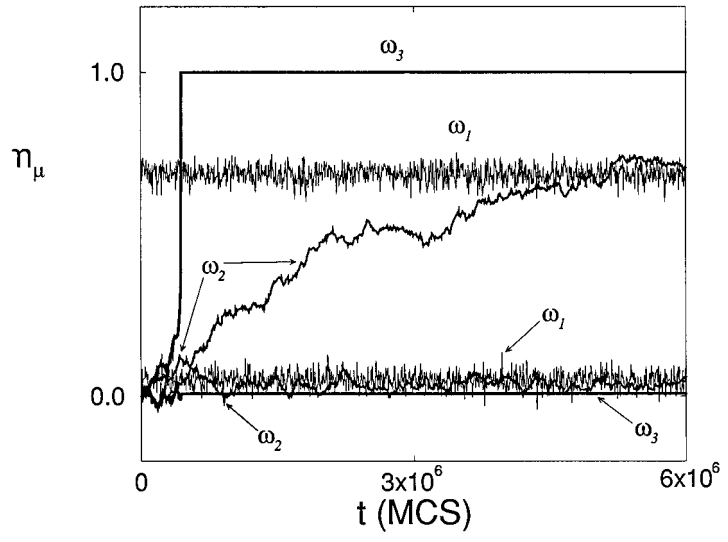

Fig. 8. Evolution with time (MC steps) of the normalized overlap $m_\mu(\mathbf{s})$ for $N=2500$ and $\mu=1$, 2 at temperature $T=0.8$ for different models, i.e., effective rates (see Eqs. (2) and (36)), as indicated. The two noisiest horizontal behaviors (ϖ_1) are for the standard Hopfield model with the Metropolis algorithm; the line slowly increasing with time, and the other one also marked ϖ_2 are for the same model with *rule V*. The lest noisy behaviors (ϖ_3) correspond to our case with synaptic fluctuations (5) and *rule V*.

that the additive nature of (5), which allows for the existence of correlations between the fluctuations at different synapses as induced by the spatial correlations contained in the patterns ξ^μ themselves, is essential for this result. In particular, assuming that effects from different patterns are multiplicative in $f(\mathbf{J})$ as in (4), induces a simpler noise, which in a sense adds to the thermal one, and differences ensue not so dramatic, though also interesting.[2]

The above illustrates how correlated fluctuations of synapsis can notably enhance both the stability and efficacy of the retrieval process in a neural network. Figure 9 confirms the good performance of the model presented here, namely, that ϖ_3, unlike ϖ_1, leads to saturation and induces a high level of robustness. The evolutions here always begin with a state obtained by perturbing greatly any of the memorized (random) patterns. Figure 9(a) shows that ϖ_3 generally leads to the "right" pattern for $T=0.6$. Further decreasing of T increases the relaxation time, even importantly, but no other qualitative effects are evident. Figure 9(b) shows the corresponding result for the Hopfield case ϖ_1. This system is much less efficient in recognizing the right pattern and, eventually, desestabilizes after some,

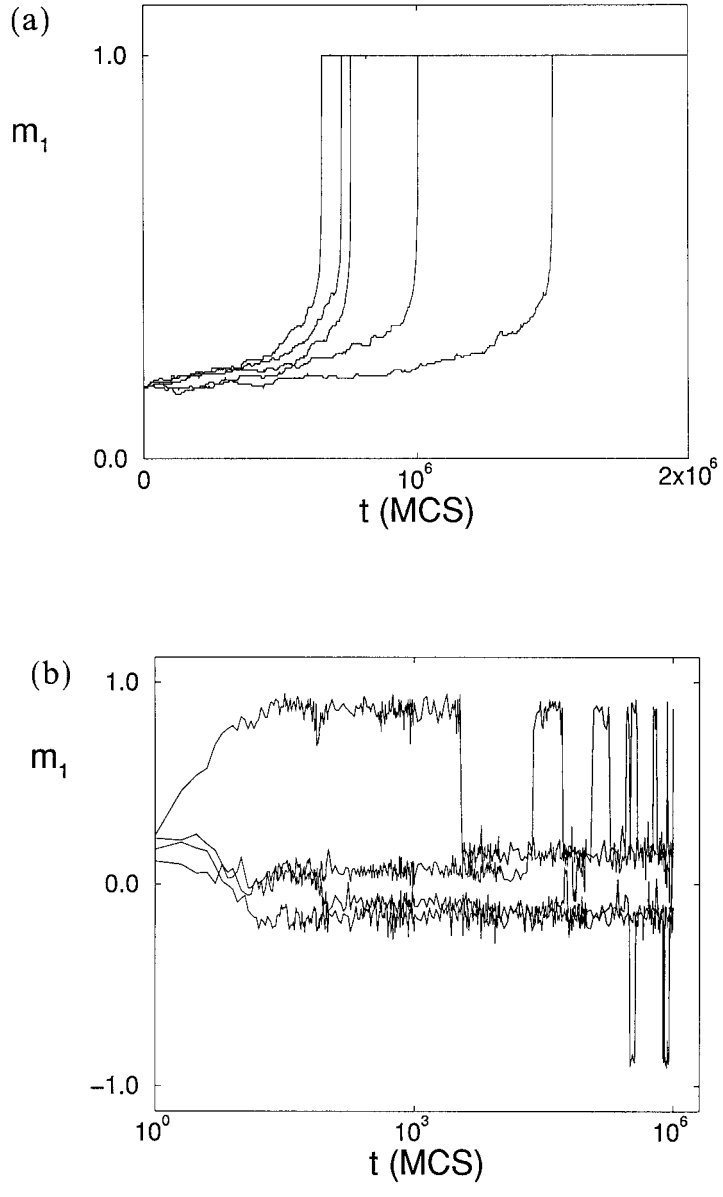

Fig. 9. This shows independent evolutions at $T=0.6$ for $N=400$ and $P=10$ (random) memorized patterns starting with the same initial state. This is obtained after perturbing by a 18% one of the given, memorized patterns. For ϖ_3 (a) and ϖ_1 (b). This illustrates that pattern recognition is also notably improved in the presence of correlated fluctuations of synapses as in (5).

relatively short time (note that time in Fig. 9(b) is in logarithmic scale in order to show the details of the early evolution).

7. DISCUSSION

The idea that, in addition to thermal noise, some sort of synaptic variations during neuronal activity are essential to the properties of biological neural networks has recently revived, because of a number of different observations in biology, physiology and psychology (see references in Section 1). Our analytical and numerical studies of a simple model that allows for a systematic study of the influence of such variations on emergent properties seems to confirm that belief. The basic model that we have analyzed in this paper is a kinetic generalization of familiar neural networks. That is, our system belongs to a class of variations of the Hopfield–Hebb network that try to capture essential features of nature (see refs. 24–29, for instance). However, a similar role of synaptic variations should probably be expected for other models.

An important feature of our model is that it evolves by competing dynamics which, in general, induces nonequilibrium steady states, the competition being between synapse and neuron variations. The simplest case of interest assumes that the neuronal configuration evolves according to Eq. (1) with the effective rate (2). This represents synapsis that, besides a —relatively slow, or previous—learning plasticity process, undergo rapid random fluctuations, i.e., synaptic intensities vary on a time scale much smaller than that for neuronal activity. (Note that—as it is implied by the results in ref. 30, for instance—the system would behave quite differently for neurons evolving much faster than synapses.) In this paper we report on synaptic fluctuations that have distributions $f(\mathbf{J})$ as given in (5), which in a way respects the spatial correlations that characterize the stored patterns. This induces full nonequilibrium behavior, as it occurs when a system is acted on by a non-Hamiltonian agent, unlike the choice (4) that we analyzed in ref. 2. We also conclude that such sort of apparent noise notably increases the efficiency in transmitting the signal.

Our analytical results involve a mean-field assymption, and they concern the case of finite P in the thermodynamic limit $N \to \infty$. We present strong evidence, however, that our conclusions are not affected by these restrictions; see Figs. 1(a), 5 and 6, for instance. In fact, the ratio P/T is more relevant in our model than P/N, as discussed above. For certain dynamical rules that are familiar from related studies,[19] the only (locally) stable solution in the model is a mixture state that has nonzero overlaps with any of the P stored patterns. Therefore, the system does not exhibit in this case associative memory. However, associative memory holds for a

different rate (*rule V*), namely, (pure) Mattis states occur for $T < \tilde{T}(1, P)$ such that $\tilde{T}(1, P < 3) = T_c$; see Figs. 1 to 3. For large enough T, only the trivial solution exists in such a way that T_c and $\tilde{T}(1, P)$ correspond to (nonequilibrium) continuous and discontinuous phase transitions, respectively; these transitions are between a paramagnetic-like phase without associative memory at high temperature, and a low-temperature ferromagnetic-like phase exhibiting this property. Another principal fact is that the discontinuity at $\tilde{T}(1, P)$ allows for *large* (close to either $+1$ or -1) overlaps for the interesting case of large values of P.

Unlike for the ordinary Hopfield case, our model does not show below $T = 0.46$ locally stable mixture states, which importantly hamper the performance of Hopfield networks at low temperature. Consequently, the error when recovering any of the stored patterns, defined as $\frac{1}{2}(1 - m_\mu)$, rapidly decreases towards zero in our model with increasing P for given T, and it remains bounded for given P as T ($< T_c$) is increased, going to zero as P becomes large enough. This behavior is illustrated in Fig. 4, which contains a comparison with the Hopfield case (in this case, the same error is independent of P at given T, and increases without bound as $T = 1$ is approached). Our model may also be worked out for asymmetric synapses; see Fig. 7; it ensues that associative memory depends on the value for the asymmetry parameters in (29). Monte Carlo simulations allow for further comparisons with some related models, and confirm and extend the analytical results; see Figs. 8 and 9. Further study of the consequences of synaptic fluctuations on the processing power of a neural network is strongly suggested.

ACKNOWLEDGMENTS

This work was supported by the Ministerio de Educación y Cultura, PB97-0842, and Junta de Andalucía.

REFERENCES

1. J. J. Hopfield, *Proc. Natl. Acad. Sci. USA* **79**:2554 (1982).
2. J. J. Torres, P. L. Garrido, and J. Marro, *J. Phys. A* **30**:7801 (1997).
3. C. R. Noback and R. J. Demarest, *The Human Nervous System: Basic Principles of Neurobiology* (McGraw-Hill, New York, 1975).
4. B. Müller and J. Reinhardt, *Neural Networks, An Introduction* (Springer-Verlag, Berlin, 1990).
5. P. Peretto, *An Introduction to the Modeling of Neural Networks* (Cambridge University Press, Cambridge, 1992).
6. D. Ferster, *Science* **273**:1812 (1996).
7. N. Otmakhov, A. M. Shirke, and R. Malinow, *Neuron* **10**:1101 (1993).

8. K. E. Sorra and K. M. Harris, *J. Neurosci.* **13**:3736 (1993).
9. A. J. Mandell and K. A. Selz, *J. Stat. Phys.* **70**:355 (1993).
10. C. F. Stevens and Y. Wang, *Nature* **371**:704 (1994).
11. Y. Goda and C. F. Stevens, *Proc. Nat. Acad. Sci. USA* **91**:12942 (1994).
12. K. J. Stratford, K. Tarczy-Hornoch, K. A. C. Martin, N. J. Bannister, and J. J. B. Jack, *Nature* **382**:258 (1996).
13. D. K. Smetters and A. Zador, *Current Biology* **6**:1217 (1996).
14. F. Moss, *Phys. World* **10**:15 (1997).
15. J. von Neummann, in *Cerebral Mechanics of Behavior*, L. A. Jeffres, ed. (Wiley, New York, 1951).
16. J. Buhmann and K. Schulten, *Biol. Cybern.* **56**:313 (1987).
17. H. Liljenström and X. B. Wu, *Int. J. Neural Systems* **6**:19 (1995).
18. W. L. Ditto and F. Moss, short report in *APS News* **6**, No. 5 (May 1997).
19. J. Marro and R. Dickman, *Nonequilibrium Phase Transitions in Lattice Models* (Cambridge University Press, Cambridge, 1999).
20. D. O. Hebb, *The Organization of Behavior: A Neurophysiological Theory* (Wiley, New York, 1949).
21. J. Marro, P. L. Garrido, and J. J. Torres, *Phys. Rev. Lett.* **81**:2827 (1998).
22. D. C. Mattis, *Phys. Lett. A* **56**:421 (1976).
23. L. Elsgoltz, *Ecuaciones Diferenciales y Cálculo Variacional* (Mir, Moscow, 1977).
24. D. J. Amit, H. Gutfreund, and M. Sompolinsky, *Phys. Rev. A* **32**:1007 (1985).
25. B. Derrida, E. Gardner, and A. Zippelius, *Europhys. Lett.* **4**:167 (1987).
26. H. Gutfreund and M. Mezard, *Phys. Rev. Lett.* **61**:235 (1988).
27. F. A. Tamarit and E. M. F. Curado, *J. Stat. Phys.* **62**:473 (1991).
28. D. Horn, *Physica A* **200**:594 (1993).
29. C. R. Da Silva, F. A. Tamarit, and E. M. F. Curado, *Int. J. Mod. Phys. C* **7**:43 (1996).
30. A. C. C. Coolen, R. W. Penney, and D. Sherrington, *Phys. Rev. B* **48**:16116 (1993); *J. Phys. A* **26**:3681 (1993).